



## Lattice with vacancies: elastic fields and effective properties in frameworks of discrete and continuum models

V. A. Kuzkin, A. M. Krivtsov, E. A. Podolskaya & M. L. Kachanov

To cite this article: V. A. Kuzkin, A. M. Krivtsov, E. A. Podolskaya & M. L. Kachanov (2016): Lattice with vacancies: elastic fields and effective properties in frameworks of discrete and continuum models, Philosophical Magazine, DOI: [10.1080/14786435.2016.1167979](https://doi.org/10.1080/14786435.2016.1167979)

To link to this article: <http://dx.doi.org/10.1080/14786435.2016.1167979>



Published online: 08 Apr 2016.



Submit your article to this journal [↗](#)



View related articles [↗](#)



View Crossmark data [↗](#)

# Lattice with vacancies: elastic fields and effective properties in frameworks of discrete and continuum models

V. A. Kuzkin<sup>a,b</sup>, A. M. Krivtsov<sup>a,b</sup>, E. A. Podolskaya<sup>a,b</sup> and M. L. Kachanov<sup>b,c</sup>

<sup>a</sup>Institute for Problems in Mechanical Engineering, RAS, St. Petersburg, Russia; <sup>b</sup>Department of Theoretical and Applied Mechanics, Peter the Great St. Petersburg Polytechnic University, St. Petersburg, Russia;

<sup>c</sup>Department of Mechanical Engineering, Tufts University, Medford, MA, USA

## ABSTRACT

Linear elastic deformation of the two-dimensional triangular lattice with multiple vacancies is considered. Closed-form analytical expressions for displacement field in the lattice with doubly periodic system of vacancies are derived. Effective elastic moduli are calculated. The results are compared with the ones obtained by molecular dynamics simulations of a lattice with random distribution of vacancies. At low vacancy concentrations, less than 4%, random and periodic distributions of vacancies produce the same effect on elastic moduli. One of the main goals is to examine the possibilities and limitations of modelling of the lattice with vacancies by an elastic continuum with holes. It is found that the effective elastic properties are modelled adequately, provided the shape of the holes is chosen appropriately. On the contrary, the strain field, in particular, strain concentration differs significantly.

## ARTICLE HISTORY

Received 2 February 2016  
Accepted 15 March 2016

## KEYWORDS

Triangular lattice; vacancy; displacement fields; effective elastic properties; shape factors; local fields; strain concentration; doubly periodic problem

## 1. Introduction

The influence of point defects on physical properties of crystals is a long-standing problem in mechanics and physics of solids. This problem has been considered in literature from both continuum and discrete points of view. Foundations of continuum theory of lattice defects have been developed in pioneering works of Eshelby [1,2]. In continuum mechanics, such defects are modelled as pores in a homogeneous elastic medium, and continuum mechanics tools are used for calculation of displacement fields [1], elastic interaction of defects [2], effective properties of imperfect crystals [3], etc. Although the continuum mechanics modelling is expected to be appropriate for the effective properties [4], it may become inadequate at microscale, in particular, near vacancies, where the discreteness plays important role [5,6]. For example, Krivtsov and Morozov [7] have shown that the effect of discreteness is significant even in the absence of surface tension [8]. Examination of these issues is the main motivation for the present work.

One of the first attempts to solve the problem in the discrete formulation was made by Kanzaki [9], who has developed foundations of the so-called lattice statics method. Kanzaki considered a periodic cell in FCC crystal containing a vacancy at the centre of the cell. The effect of vacancy is simulated by applying forces to atoms that simulate

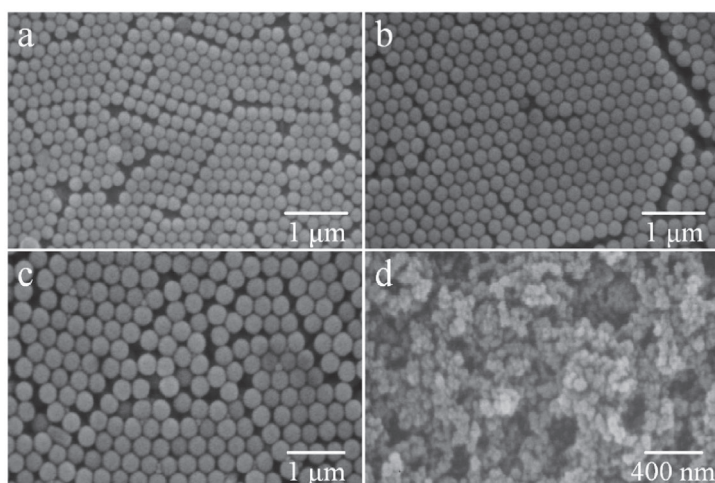


**Figure 1.** Scanning electron microscopy images of polystyrene (PS) colloids and carbon black nanoparticles (CB-NPs) used to prepare hybrid colloidal crystal coatings: (a) 190 nm PS colloids; (b) 217 nm PS colloids; (c) 308 nm PS colloids; (d) 33 nm CB-NPs. *Reprinted with permission from [29].*

interatomic interactions with both the nearest and farther lying atoms. Then, equations of lattice statics in harmonic approximation are solved using discrete Fourier transform (DFT). Kanzaki approach and its modifications [10] have been widely used for studying vacancies and interstitials in various metals [11–16] and alloys [17]. Generalisation of lattice statics approach for anharmonic interactions has been developed in papers [18–20].

An alternative discrete approach based on lattice Green's function has been proposed by Tewary [21], who showed that this approach is equivalent to the lattice statics method, but is computationally simpler. The Green's function has been calculated for a variety of systems including triangular [22,23], diamond-like [24], graphene [25] and hexagonal close-packed lattices [26].

The two-dimensional modelling taken in the present work is relevant for a variety of 2-D materials, such as 2-D colloids [27–30] (see e.g. Figure 1), boron nitride [31], etc. that have become available due to recent advances in technology. Effective elastic properties and displacement fields in carbon nanosheets having ideal hexagonal structure were identified in [31]. Displacement fields caused by point defects in two-dimensional colloidal crystals were studied in papers [27,28]. Authors have adopted Ewald summation technique for solution of continuum elasticity problems with periodic boundary conditions. It has been demonstrated that the continuum theory loses accuracy in close vicinity of defects. In the case of triangular lattice, the method of discrete Green's function has been used for calculation of the effective elastic moduli [23]. However, explicit analytical expressions for displacement fields around vacancies, in the discrete formulation, have not been given in the above-mentioned works.

The present work focuses on elastic deformation of a triangular lattice with periodic array of vacancies. Firstly, the displacements of all particles are expressed in terms of a mean strain; secondly, using Hooke's law and defining the mean traction as the mean force acting on the cell boundary (that, in turn, is a function of displacements), the effective moduli are calculated that can be used further to find the relation between displacements and

stresses applied at infinity. This approach differs from Kanzaki and lattice Green's function approaches, where the displacements are expressed in terms of interatomic forces. Note that our approach constitutes a discrete analogue of doubly periodic problem in continuum elasticity [32–35]. Analytical treatment of the *discrete doubly periodic problem* is based on the exact solution of corresponding partial difference equations. Closed-form expressions for particle displacements in the mentioned discrete doubly periodic problem are obtained by the use of DFT.

The main focus of the present work is to examine the following issue: 'to what extent a vacancy in triangular lattice can be modeled by a pore (hole) in elastic continuum media and what the pore shape should be?' The equivalence is considered from two points of view: (i) displacement field around a vacancy and (ii) effective elastic properties of a lattice with vacancies.

## 2. Analytical solution for triangular lattice with a doubly periodic system of vacancies

We present an analytical solution for the displacement field in a triangular lattice [36] with a doubly periodic system of vacancies subjected to stresses applied at infinity (Figure 2). The periodic cell (sometimes referred to as supercell [37]) has the shape of a rhombus with  $2N + 1$  particles on each side. The vacancies are located at rhombi centres. We assume that each atom interacts only with the nearest neighbours (the justification being that interatomic forces decrease very rapidly with distance), and the interaction forces are modelled by linear elastic springs (as justified by the small deformations formulation). The atom displacements are calculated in terms of the mean deformation of the cell. The displacements can be recalculated in terms of applied stresses with the use of the effective elastic moduli, introduced in Section 3.

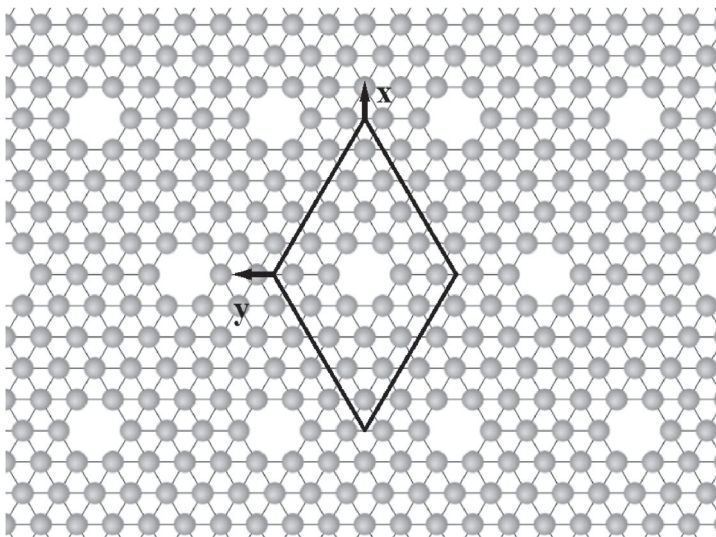


**Figure 2.** Triangular lattice with a doubly periodic system of vacancies,  $N = 2$ . Solid line shows the periodic cell.

## 2.1. Equilibrium equations for a lattice with vacancy

Consider triangular lattice consisting of identical particles connected with the nearest neighbours by linear springs. Infinitesimal deformations of the lattice are considered. Equilibrium equations for the lattice are written as partial difference equations [38].

We introduce unit vectors  $\mathbf{e}_u$ ,  $\mathbf{e}_v$ ,  $\mathbf{e}_w$  that correspond to the bonds' directions in the lattice:

$$\mathbf{e}_u = \frac{\sqrt{3}}{2}\mathbf{i} + \frac{1}{2}\mathbf{j}, \quad \mathbf{e}_v = -\frac{\sqrt{3}}{2}\mathbf{i} + \frac{1}{2}\mathbf{j}, \quad \mathbf{e}_w = \mathbf{e}_u + \mathbf{e}_v, \quad (1)$$

where  $\mathbf{i}, \mathbf{j}$  are unit vectors of 2-D Cartesian coordinate system and correspond to the  $x$ - and  $y$ -axis, respectively (see Figure 2);  $\mathbf{I} = \mathbf{ii} + \mathbf{jj} = \frac{2}{3}(\mathbf{e}_u\mathbf{e}_u + \mathbf{e}_v\mathbf{e}_v + \mathbf{e}_w\mathbf{e}_w)$  is the two-dimensional unit tensor. A displacement vector  $\mathbf{u}$  can be represented as:

$$\mathbf{u} = \frac{2}{3}(u\mathbf{e}_u + v\mathbf{e}_v + w\mathbf{e}_w), \quad u = \mathbf{u} \cdot \mathbf{e}_u, \quad v = \mathbf{u} \cdot \mathbf{e}_v, \quad w = \mathbf{u} \cdot \mathbf{e}_w = u + v. \quad (2)$$

We introduce two indices  $n, m$  that enumerate the particles so that their position vectors are:

$$\mathbf{r}^{n,m} = a(n\mathbf{e}_u + m\mathbf{e}_v), \quad (3)$$

where  $a$  is the equilibrium distance between the nearest neighbours. Consider the second-order partial difference operators  $\Delta_u, \Delta_v, \Delta_w$  which correspond to the directions  $u, v, w$ :

$$\begin{aligned} \Delta_u(\mathbf{u}^{n,m}) &= \mathbf{u}^{n+1,m} - 2\mathbf{u}^{n,m} + \mathbf{u}^{n-1,m}, & \Delta_v(\mathbf{u}^{n,m}) &= \mathbf{u}^{n,m+1} - 2\mathbf{u}^{n,m} + \mathbf{u}^{n,m-1}, \\ \Delta_w(\mathbf{u}^{n,m}) &= \mathbf{u}^{n+1,m+1} - 2\mathbf{u}^{n,m} + \mathbf{u}^{n-1,m-1}. \end{aligned} \quad (4)$$

These operators are discrete analogues of partial derivatives with respect to the spatial coordinates used in continuum theory. The equilibrium equations for the particle  $n, m$  having six nearest neighbours are the following:

$$\Delta_u u^{n,m} \mathbf{e}_u + \Delta_v v^{n,m} \mathbf{e}_v + \Delta_w w^{n,m} \mathbf{e}_w = 0. \quad (5)$$

Hereafter, there is no summation over repeated indices. The projections of this equation on the basis vectors  $\mathbf{e}_u, \mathbf{e}_v$  yield:

$$\begin{aligned} \Delta_u u^{n,m} + \Delta_w (u^{n,m} + v^{n,m}) &= 0, \\ \Delta_v v^{n,m} + \Delta_w (u^{n,m} + v^{n,m}) &= 0. \end{aligned} \quad (6)$$

Equation (6) describe the equilibrium of a particle 'in the bulk' (having six nearest neighbours) in the absence of body forces.

Now, consider a single vacancy at  $\mathbf{r}^{0,0} = 0$ . The particles surrounding the vacancy have only five nearest neighbours. Therefore, their equilibrium equations differ from those for particles that are not adjacent to the vacancy. In order to write the equilibrium equations for all particles in a unified way, the following 'bond-elimination' difference operators are introduced:

$$\begin{aligned}
 \beta_u^\pm \mathbf{u}^{n,m} &= \delta^{n,m}(\mathbf{u}^{n\pm 1,m} - \mathbf{u}^{n,m}) + \delta^{n\mp 1,m}(\mathbf{u}^{n\mp 1,m} - \mathbf{u}^{n,m}), \\
 \beta_v^\pm \mathbf{u}^{n,m} &= \delta^{n,m}(\mathbf{u}^{n,m\pm 1} - \mathbf{u}^{n,m}) + \delta^{n,m\mp 1}(\mathbf{u}^{n,m\mp 1} - \mathbf{u}^{n,m}), \\
 \beta_w^\pm \mathbf{u}^{n,m} &= \delta^{n,m}(\mathbf{u}^{n\pm 1,m\pm 1} - \mathbf{u}^{n,m}) + \delta^{n\mp 1,m\mp 1}(\mathbf{u}^{n\mp 1,m\mp 1} - \mathbf{u}^{n,m}).
 \end{aligned} \tag{7}$$

Here  $\delta^{n,m} = 1$  for  $n = m = 0$ , and  $\delta^{n,m} = 0$  for the other cases. Then, the equilibrium equations for any particle  $\{n, m\}$  in a lattice with vacancy have the form:

$$\begin{aligned}
 (\Delta_u - \beta_u^+ - \beta_u^-)u^{n,m} + (\Delta_w - \beta_w^+ - \beta_w^-)(u^{n,m} + v^{n,m}) &= 0, \\
 (\Delta_v - \beta_v^+ - \beta_v^-)v^{n,m} + (\Delta_w - \beta_w^+ - \beta_w^-)(u^{n,m} + v^{n,m}) &= 0.
 \end{aligned} \tag{8}$$

The effect of bond-elimination operators is identical to bonds of negative stiffness.

Thus, we have obtained the unified form (8) of the equilibrium equation for the triangular lattice with a single vacancy. These equations together with the periodic boundary conditions will be used for calculation of the displacement field.

## 2.2. Displacement field in a triangular lattice with doubly periodic system of vacancies

Equilibrium Equation (8) can be solved analytically for a lattice with doubly periodic system of vacancies (see Figure 2). We denote the mean strain tensor of the periodic cell, induced by remotely applied stress, by  $\boldsymbol{\varepsilon}$  and express particles' displacements in terms of  $\boldsymbol{\varepsilon}$ . In the present section, the displacements of particles are calculated and compared with the solution of continuum Kirsch problem.

We represent displacement of a particle as a sum of a doubly periodic part  $\tilde{\mathbf{u}}^{n,m}$  and a linear function of the strain tensor  $\boldsymbol{\varepsilon}$  (quasi-periodicity [34]):

$$\mathbf{u}^{n,m} = \tilde{\mathbf{u}}^{n,m} + a\boldsymbol{\varepsilon} \cdot (n\mathbf{e}_u + m\mathbf{e}_v), \quad \tilde{\mathbf{u}}^{n+\alpha(2N+1),m+\beta(2N+1)} = \tilde{\mathbf{u}}^{n,m}, \tag{9}$$

where  $\alpha$  and  $\beta$  denote the cell's number. This expression is substituted into equilibrium Equations (8). The resulting equations are solved with respect to  $\tilde{\mathbf{u}}^{n,m}$  using DFT. The DFT allows one to satisfy periodicity conditions (9) automatically. The solution procedure in detail is presented in Appendix 1. The general solution is rather cumbersome, so in the present section, we consider only several special cases.

### 2.2.1. Volumetric mean strain

Consider the case of volumetric mean strain  $\boldsymbol{\varepsilon} = \varepsilon\mathbf{I}$ . We focus on the effect of elastic interaction of vacancies. This effect is analysed by comparing the solution for infinite cell (one vacancy) with the solution for a cell of finite size. Solution for infinite cell will be denoted by subscript  $\infty$ . The displacements of particles have the form (see Appendix 2 for derivation):

$$u^{n,m} = v^{m,n} = a\varepsilon \left( n - \frac{m}{2} - \frac{G^{n,m}}{1 + G^{1,0}} \right), \tag{10}$$

where

$$G^{n,m} = \frac{1}{2(2N+1)^2} \sum_{s,p=-N}^N g(s\theta, p\theta) \sin((sn+pm)\theta), \quad \theta = \frac{2\pi}{2N+1},$$

$$g(x, y) = \frac{\sin y \sin^2 \frac{x}{2} - \sin x \sin^2 \frac{y}{2}}{\sin^2 \frac{x}{2} \sin^2 \frac{y}{2} + \sin^2 \frac{x}{2} \sin^2 \frac{x+y}{2} + \sin^2 \frac{y}{2} \sin^2 \frac{x+y}{2}}. \quad (11)$$

Note that the sum in formula (11) converges quite fast with the increase in  $N$ . For a particle adjacent to the vacancy, the convergence is very fast and the limiting value  $N \rightarrow \infty$  is practically reached at  $N \sim 10$  (see Figure 3(a)). In the case of infinite cell (one vacancy only),  $G^{n,m}$  is given by the integral:

$$G_{\infty}^{n,m} = \frac{1}{8\pi^2} \int_{-\pi}^{\pi} \int_{-\pi}^{\pi} g(x, y) \sin(nx + my) dx dy. \quad (12)$$

Formulae (10)–(12) give exact expressions for particle displacements.

Consider displacements of particles forming the vacancy. Taking the limit  $N \rightarrow \infty$  (infinite cell), formulae (10)–(12) yield:

$$u_{\infty}^{1,0} \approx 1.642a\varepsilon. \quad (13)$$

Here,  $a\varepsilon$  is the displacement of the same particles in the case of perfect crystal (no vacancy).

We estimate the effect of elastic interaction of vacancies by comparing total displacements of particles near the vacancy at  $N = 1$  (minimal cell size) and  $N \rightarrow \infty$  (one vacancy in infinite crystal). Calculations show that the difference is about 20% (Figure 3(a)).

We now compare the obtained results with results of the elasticity theory. Displacement field in a plate with<sup>1</sup>  $\nu_0 = 1/3$  containing a circular hole of radius  $R$  loaded by remotely applied hydrostatic stress  $\sigma_0$  (Kirsch problem) has the form:

$$\mathbf{u} \cdot \mathbf{e}_r = \varepsilon r + 2 \frac{\varepsilon R^2}{r}, \quad \varepsilon = \frac{\sigma_0}{2K_0}, \quad (14)$$

where  $r$  is the distance from the hole centre,  $\mathbf{e}_r = \mathbf{r}/r$ ,  $K_0$  is the bulk modulus.

The radial component of particle displacements in a lattice is represented in a similar form:

$$\mathbf{u}^{n,m} \cdot \mathbf{e}_r = \varepsilon r + \tilde{\mathbf{u}}^{n,m} \cdot \mathbf{e}_r. \quad (15)$$

The first terms in formulae (14), (15) for continuum and discrete displacement fields coincide. Let us check at what distance from the vacancy the second part  $\tilde{\mathbf{u}}^{n,m} \cdot \mathbf{e}_r$  can be approximated by a function  $A/r$ .

Figure 3(b) shows the radial component  $\tilde{\mathbf{u}}^{n,m} \cdot \mathbf{e}_r$  as a function of the dimensionless distance  $r/a$  from the vacancy for  $N = 100$ . Without loss of generality, it is assumed that  $\varepsilon = 1$ . Circles denote the analytical discrete solution. Continuous curve denotes the corresponding continuum dependency;  $A = 0.604a^2$ , and it is determined with 0.5% accuracy. It is seen that for  $r/a > 10$ , the displacements of the particles approach the continuum curve. According to formula (14), the coefficient  $A$  determines the equivalent radius of the vacancy:

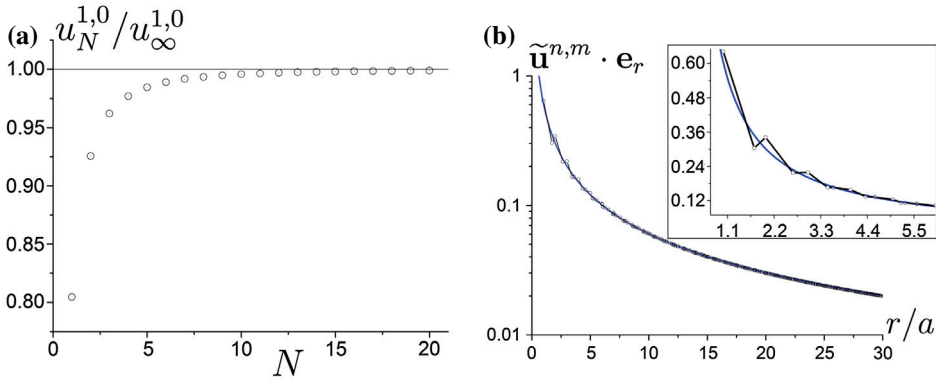


**Figure 3.** Volumetric mean strain. (a) The total displacement of particle 1,0 forming the vacancy ( $n = 1$ ,  $m = 0$ ) as a function of the periodic cell size  $N$ . (b) The radial displacement  $\tilde{\mathbf{u}}^{n,m} \cdot \mathbf{e}_r$  as a function of the dimensionless distance  $r/a$  from the vacancy ( $N = 100$ ).

$$R \approx 0.55a. \quad (16)$$

The main difference between the discrete and continuum solutions is demonstrated in the offset figure in Figure 3(b). In the vicinity of vacancy, the dependence  $u_r(r/a)$  is *non-monotonic*. This shows inadequacy of continuum modelling of the lattice in the vicinity of the defect. Similar effect is observed in *ab initio* calculations of displacements around a vacancy in nickel [39]. Further evidence of inadequacy of such modelling is given in Section 6, in the context of strain concentration near the vacancy.

### 2.2.2. Biaxial mean strain

Consider the biaxial mean strain of the lattice, i.e. the mean strain tensor has the form:

$$\boldsymbol{\varepsilon} = \frac{\varepsilon_{xx}}{3}(\mathbf{e}_u - \mathbf{e}_v)(\mathbf{e}_u - \mathbf{e}_v) + \varepsilon_{yy}\mathbf{e}_w\mathbf{e}_w, \quad \varepsilon_u = \varepsilon_v = \frac{3\varepsilon_{xx} + \varepsilon_{yy}}{4}, \quad \varepsilon_w = \varepsilon_{yy}. \quad (17)$$

In the Appendix 3, it is shown that the doubly periodic part of the displacement field has the form:

$$\begin{aligned} \tilde{\mathbf{u}}^{n,m} &= \tilde{\mathbf{v}}^{m,n} = H^{n,m}(a\varepsilon_u + \tilde{u}^{1,0}) + K^{n,m}(a\varepsilon_w + \tilde{w}^{1,1}), \\ \tilde{u}^{1,0} &= a \frac{(H^{1,0}(1 - 2K^{1,1}) + 2H^{1,1}K^{1,0})\varepsilon_u + K^{1,0}\varepsilon_w}{(1 - H^{1,0})(1 - 2K^{1,1}) - 2K^{1,0}H^{1,1}}, \\ \tilde{w}^{1,1} &= 2a \frac{H^{1,1}\varepsilon_u + (K^{1,1}(1 - H^{1,0}) + H^{1,1}K^{1,0})\varepsilon_w}{(1 - H^{1,0})(1 - 2K^{1,1}) - 2K^{1,0}H^{1,1}}, \end{aligned} \quad (18)$$

where

$$\begin{aligned} H^{n,m} &= \frac{1}{2(2N+1)^2} \sum_{s,p=-N}^N \frac{\sin((sn+pm)\theta)}{D^{s,p}} \left( \sin s\theta \sin^2 \frac{p\theta}{2} \right. \\ &\quad \left. + \sin^2 \frac{(s+p)\theta}{2} (\sin s\theta - \sin p\theta) \right), \end{aligned} \quad (19)$$



$$K^{n,m} = \frac{1}{2(2N+1)^2} \sum_{s,p=-N}^N \frac{\sin((sn+pm)\theta)}{D^{s,p}} \sin((s+p)\theta) \sin^2 \frac{p\theta}{2},$$

$$D^{s,p} = \sin^2 \frac{s\theta}{2} \sin^2 \frac{p\theta}{2} + \sin^2 \frac{p\theta}{2} \sin^2 \frac{(s+p)\theta}{2} + \sin^2 \frac{s\theta}{2} \sin^2 \frac{(s+p)\theta}{2}.$$

In the case of the infinite crystal  $N \rightarrow \infty$ , the sums in formulae (19) can be replaced by integrals, similar to (12). In the next section, these expressions are employed for calculation of the effective elastic moduli. In Section 6, they are used to find concentrations of the local fields near vacancies.

### 3. Effective elastic moduli of a triangular lattice with doubly periodic system of vacancies

Consider the influence of vacancies on the effective elastic properties of the crystal. Since the geometrical pattern of the microstructure has the hexagonal symmetry, the effective elastic properties are isotropic. To determine the effective bulk modulus  $K$  and shear modulus  $\mu$ , it is sufficient to consider two cases of the mean strain: hydrostatic strain  $\varepsilon_{xx} = \varepsilon_{yy}$  and deviatoric strain  $\varepsilon_{xx} = -\varepsilon_{yy}$ . Using Hooke's law, we express the effective elastic moduli in terms of the mean traction  $\mathbf{T}$  on the periodic cell boundary with normal  $\mathbf{n}$ :

$$K = \frac{1}{2} \frac{\mathbf{T} \cdot \mathbf{n}}{\mathbf{n} \cdot \boldsymbol{\varepsilon} \cdot \mathbf{n}} \Big|_{\varepsilon_{xx}=\varepsilon_{yy}}, \quad \mu = \frac{1}{2} \frac{\mathbf{T} \cdot \mathbf{n}}{\mathbf{n} \cdot \boldsymbol{\varepsilon} \cdot \mathbf{n}} \Big|_{\varepsilon_{xx}=-\varepsilon_{yy}}, \quad \mathbf{n} = \frac{1}{2}(\mathbf{i} + \sqrt{3}\mathbf{j}). \quad (20)$$

We define the mean traction as the mean force acting on the cell boundary per unit length, i.e. interparticle distance  $a$ . Then, adding up the forces which act along the directions  $\mathbf{e}_u$  and  $\mathbf{e}_w$ , we get:

$$\mathbf{T} = T_u \mathbf{e}_u + T_w \mathbf{e}_w, \quad T_u = \frac{c}{4}(3\varepsilon_{xx} + \varepsilon_{yy}) + \frac{c}{(2N+1)a} \sum_{m=-N}^N (\tilde{u}^{-N,m} - \tilde{u}^{N,m}),$$

$$T_w = c\varepsilon_{yy} + \frac{c}{(2N+1)a} \sum_{m=-N}^N (\tilde{w}^{-N,m+1} - \tilde{w}^{N,m}). \quad (21)$$

Here,  $c$  is the bond stiffness;  $aT_u$ ,  $aT_w$  are mean forces in the bonds directed along  $\mathbf{e}_u$  and  $\mathbf{e}_w$ , respectively. The values of  $T_u$  and  $T_w$  are determined by the particles' displacements (18). Thus, the effective elastic moduli are calculated by substituting (18) and (21) into (20).

Figure 4 shows the convergence of the effective elastic constants to the values for an ideal lattice as the concentration of vacancies decreases. In Section 5, we compare the above-mentioned results with the ones obtained using the continuum theory.

### 4. Triangular lattice with random distribution of vacancies: a molecular dynamics study

We now consider the molecular dynamics (MD) simulations of the effective elastic properties of triangular lattice with vacancies. As discussed in Section 2, the interaction between

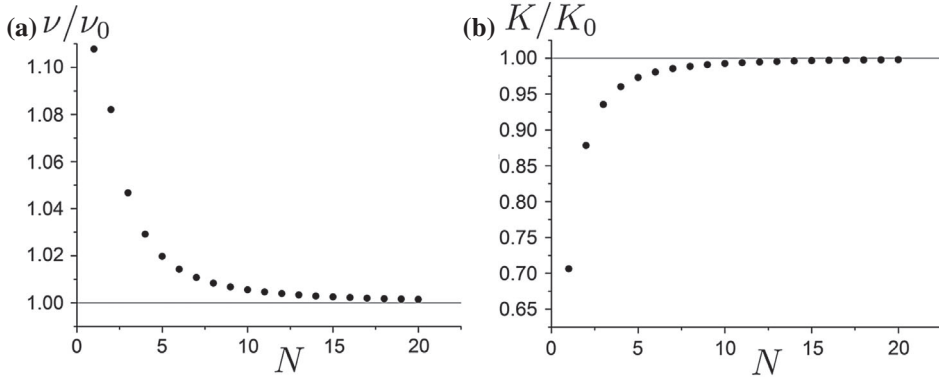


**Figure 4.** Ratios of the Poisson's ratio and bulk modulus of the lattice with doubly periodic systems of vacancies to their values for the lattice without vacancies ( $\nu_0 = 1/3$ ) as the cell size  $N$  increases (concentration of vacancies decreases).

particles is modelled by linear elastic springs of stiffness  $c$ , and only interactions between the nearest neighbours are considered. Bonds breaking and related phenomena are not considered (see [40] for more details). We use the periodic boundary conditions for the square cell containing large number of vacancies (Figure 5). From the computational point of view, it is advantageous to consider the static problem as the limiting case of dynamic problem with viscous friction as time tends to infinity. In the beginning of the simulation, the particles are attributed to random velocities uniformly distributed in a circle of radius  $\nu_0$ . Equations of motion of the particles are solved numerically using Verlet symplectic integration scheme [41].

Effective elastic moduli of the lattice with vacancies are calculated as follows. Initially, the lattice is subjected to uniform strain. In order to calculate the bulk and shear moduli, the cases  $\varepsilon_{xx} = \varepsilon_{yy}$  and  $\varepsilon_{xx} = -\varepsilon_{yy}$  are considered. In the presence of a vacancy, such state is non-equilibril. Hence, motions occur, which are then damped by viscous forces. After certain time, the motions cease, and this state is treated as the elastostatic limit of interest. Average traction vector is calculated in the cross sections with normal  $\mathbf{n} = \mathbf{j}$ . Then, bulk and shear moduli are obtained by formulae (20). The following values of parameters are used in the simulations:

$$M = 2.25 \cdot 10^4, \quad \varepsilon_{xx} = \pm \varepsilon_{yy} = \pm 10^{-5}, \quad \frac{b}{b_0} = 5 \cdot 10^{-3}, \quad \frac{\Delta t}{T_*} = 0.02, \\ \frac{\nu_0}{\nu_s} = 10^{-4}, \quad s_{\max} = 25 \cdot 10^3. \quad (22)$$

where  $M$  is the number of particles;  $\nu_s = a/T_*$ ;  $T_*$  is the period of oscillations of one particle attached to a spring of stiffness  $c$ ;  $b_0 = 2\sqrt{mc}$  is the critical viscosity coefficient;  $\Delta t$  is the time step;  $s_{\max}$  the number of integration steps. For each value of porosity, 10 calculations with various random vacancy distributions have been carried out.

The effective elastic moduli of a lattice with random distribution of vacancies are shown in Figure 6. In particular, Figure 6 demonstrates that the lattice with periodic distribution of vacancies is stiffer than the one with random distribution. Note that the dependencies are nearly linear for random distribution, whereas for periodic case, nonlinearity is visible. In

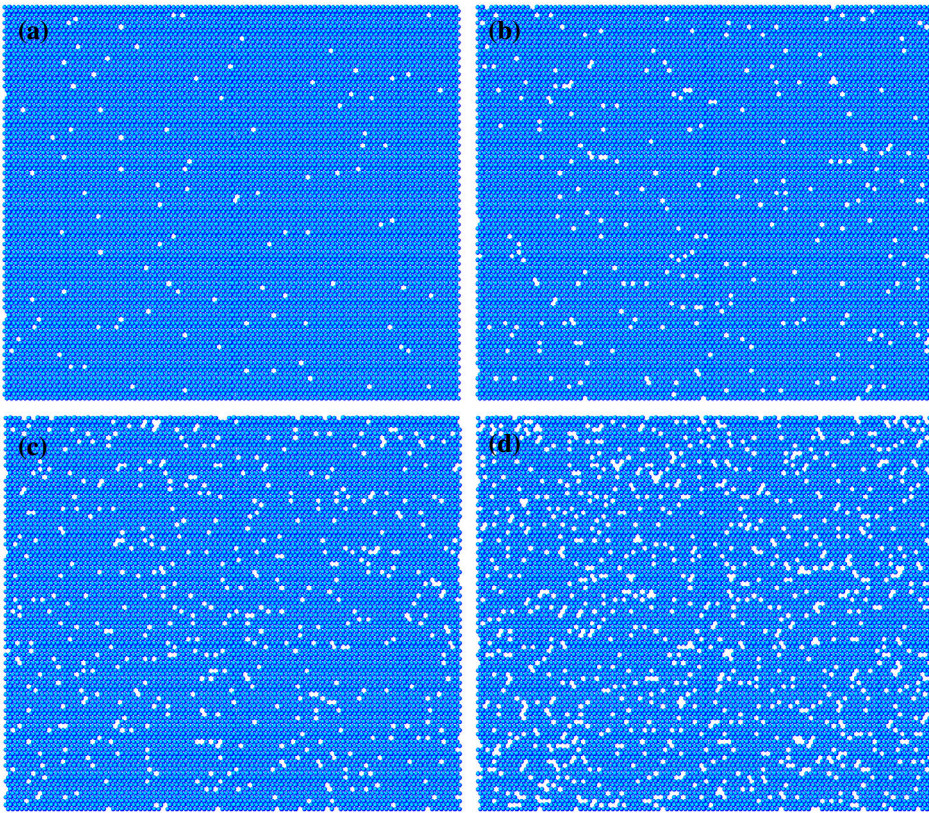


**Figure 5.** (colour online) Triangular lattice with randomly distributed vacancies. Porosity is defined as the fraction of those particles that have been removed: (a)  $p = 0.01$ , (b)  $p = 0.025$ , (c)  $p = 0.05$ , (d)  $p = 0.1$ .

Section 5, the results of MD simulations are compared with predictions of the continuum elasticity theory.

## 5. Comparison with continuum model for effective properties of triangular lattice with vacancies

We examine to what extent the lattice with vacancies can be modelled as a continuum elastic material with pores, and what shape should the pores have for adequate modelling.

For a lattice with vacancies, porosity is defined as the fraction of removed particles. For example, in doubly periodic problem,  $p = 1/(2N + 1)^2$ , where  $N$  determines the periodic cell size. In the case of continuum 2-D elasticity, porosity is defined as the area fraction of pores. Both definitions correspond to experimentally measurable quantities, in terms of specific weight.

In continuum elasticity models (see e.g. [42–45]), the effective elastic moduli depend on pore shapes, with the circular shape being the stiffest one among all shapes of given area. Figure 6 shows that the circular pore shape assumption results in poor agreement with discrete models: the discrete system is softer. This indicates that shapes other than circular have to be chosen for the best matching.

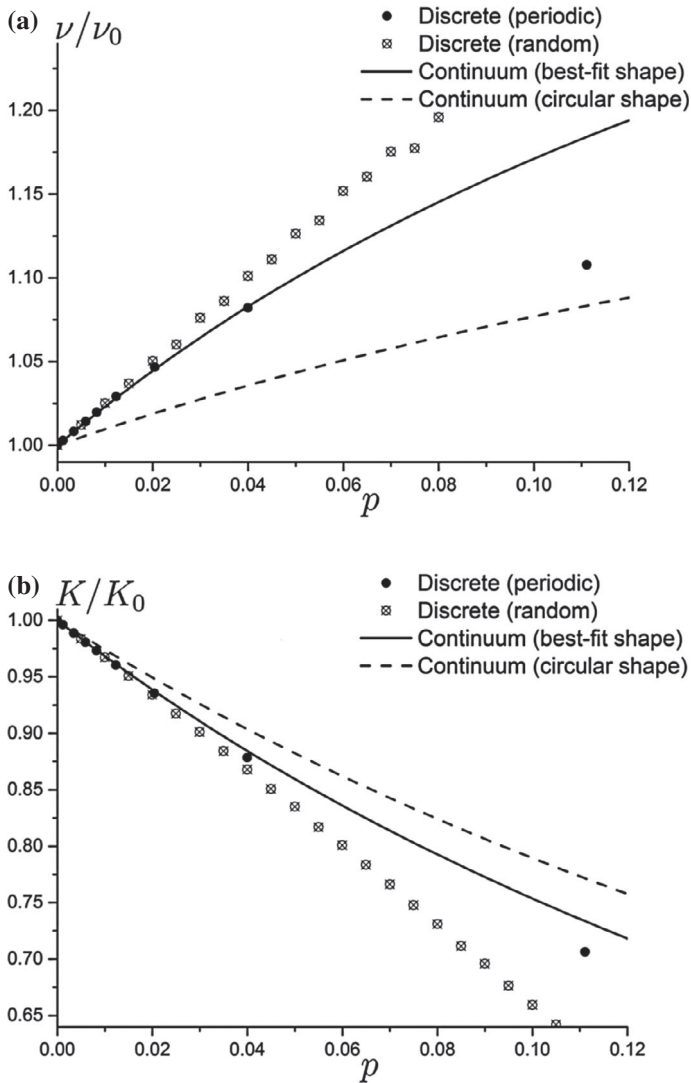


**Figure 6.** The porosity dependence of the effective elastic moduli of a triangular lattice with periodic (Section 3) and random (Section 4) distributions of vacancies: (a) the Poisson's ratio, (b) the bulk modulus. The moduli are normalised to their values in absence of vacancies. Comparison with the continuum results for best-fit shape factors (solid line) and for circular pores (dashed line).

Stiffness of a pore can be described by shape factors  $h_1, h_2$  that characterise the contribution of a pore to the overall compliances. Shape factors were derived, for a number of shapes, by Kachanov et al. [43] who also found that the factor of *concavity* substantially increases pore compliance and by Ekelinogoda and Zimmerman [44,45]. Hence, the effective elastic properties of a solid with pores depend, in addition to porosity  $p$ , on the shape factors. For a 2-D material with randomly oriented pores, the effective moduli are given by:

$$E = \frac{E_0}{1 + 2h_1p}, \quad K = \frac{K_0}{1 + 2(h_1 - h_2)p/(1 - \nu_0)},$$

$$\nu = \frac{\nu_0 + 2h_2p}{1 + 2h_1p}, \quad \mu = \frac{\mu_0}{1 + 2(h_1 + h_2)p/(1 + \nu_0)}, \quad (23)$$

where shape factors  $h_1, h_2$  for a number of polygonal shapes of varying degree of concavity were calculated in papers [43–45]. For a circle,  $h_1 = 1.5, h_2 = 0.5$ ; for other shapes,  $h_i$  are larger.

Trying to match the effective moduli given by the discrete model calculations by the moduli of an elastic plate with pores of the *circular* shape – while keeping porosity  $p$  the same as in the lattice – results in poor agreement (Figure 6). Good fit is provided by the following shape factors:  $h_1 = 2.036, h_2 = 0.810$ . Note, however, that the geometrical shape corresponding to these values is not immediately identifiable (and may not be unique). Attention should also be drawn to the increase in the Poisson's ratio with the porosity, as this behaviour is opposite to that observed for polycrystalline materials [46].

Thus, from the viewpoint of effective moduli, triangular lattice with vacancies *can* be modelled by an elastic plate with holes (that has the same porosity). However, the geometrical shape of the holes required for the best fit is not circular, and is not easily identified. Hence, for other lattice types, the best-fit shape factors of holes need to be computed anew, for each lattice type.

## 6. Inadequacy of continuum mechanics modelling of local fields

In an elastic plate with a hole, the presence of the hole leads to concentration of stresses. The stress concentration factor for a circular hole under imposed volumetric strain is equal to 2 at all points of the boundary; for other shapes, the maximal, around the boundary, concentration factor is higher. Vacancy causes similar effect; however, calculation of stress concentration factor is not straightforward, since stresses in discrete media are defined somewhat ambiguously [47,48].

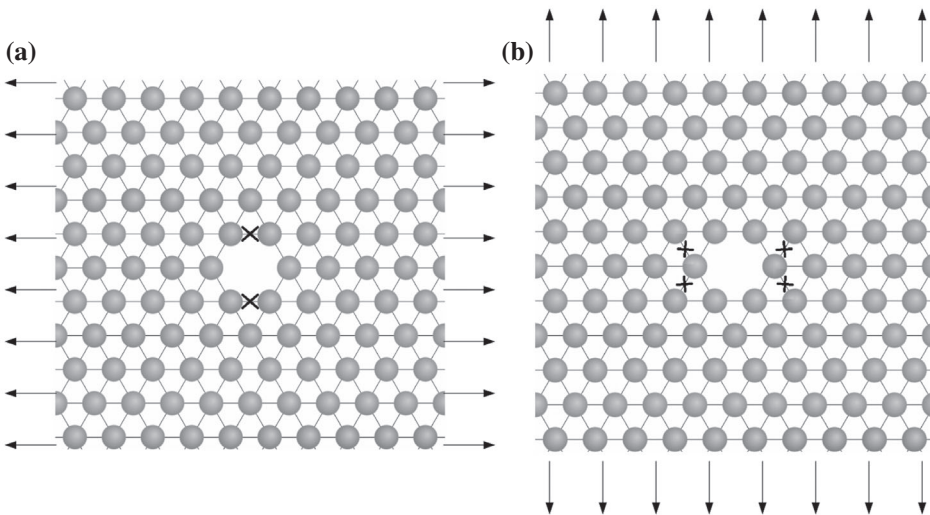


**Figure 7.** Strain concentration at uniaxial loading: (a) along the horizontal axis ( $\sigma_{0xx} = 0, \sigma_{0yy} = \sigma_0$ ), (b) along the vertical axis ( $\sigma_{0xx} = \sigma_0, \sigma_{0yy} = 0$ ). The bonds, where the maximum strain is reached, are crossed.

We define and compute the strain concentration factor,  $k$ , as the ratio of the maximal deformation of the bonds adjacent to the vacancy to the deformations of bonds at infinity. In the case of volumetric deformation, the maximum elongation is reached in the bonds that surround the vacancy. Calculating the strain concentration factor,  $k_{vol}$ , using formula (13), we get:

$$k_{vol} = \frac{u_{\infty}^{1,0}}{a\varepsilon} \approx 1.642, \quad (24)$$

that is substantially smaller than the value of 2 for the circular hole; the difference with non-circular shape(s) providing the best fit for the effective moduli will be larger.

The difference is even larger for other modes of loading. Consider, for example, uniaxial loading of the triangular lattice with vacancy in horizontal,  $y$ , and vertical,  $x$ , directions (Figure 2). The mean deformations corresponding to uniaxial stress loading in horizontal direction have the form:

$$\varepsilon_{xx} = -\nu_0\varepsilon, \quad \varepsilon_{yy} = \varepsilon, \quad \nu_0 = \frac{1}{3} \quad \Rightarrow \quad \varepsilon_u = \varepsilon_v = 0, \quad \varepsilon_w = \varepsilon. \quad (25)$$

As expected, the maximum elongation is reached in the bonds bordering the vacancy (Figure 7(a)). The strain concentration factor calculated using displacement field (18), (19) is:

$$k_y \approx 1.283, \quad (26)$$

that is much smaller than the factor of 3 in the continuum Kirsch problem for a circular hole (that is even higher for non-circular shapes).

Now, consider the uniaxial stress loading in vertical,  $x$ , direction:

$$\varepsilon_{xx} = \varepsilon, \quad \varepsilon_{yy} = -\nu_0\varepsilon \quad \Rightarrow \quad \varepsilon_u = \varepsilon_v = \frac{2}{3}\varepsilon, \quad \varepsilon_w = -\frac{1}{3}\varepsilon. \quad (27)$$

Calculating the strain concentration factor using displacement field (18), (19) we obtain:

$$k_x \approx 1.449, \quad (28)$$

that is, again, much smaller than the factor of 3 in the continuum problem.

The above examples show that the concentrations of fields near vacancies cannot be adequately modelled in the framework of the continuum elasticity theory.

## 7. Conclusions

We have shown that, from the viewpoint of the effective elastic properties, a lattice with vacancies can be modelled in the framework of 2-D elasticity (plate with holes). However, the strength characteristics and local fields – in particular, strain concentrations near vacancies – cannot be adequately modelled in the said framework. The absence of correlations between pore compliances and local fields has been noted earlier, in a different context by Ekneligoda and Zimmerman [49].

We note that hole shape factors required for the best fit are substantially different from the ones for a circle. We add that the geometrical shape corresponding to the mentioned shape factors is not easily identifiable (and may even be non-unique).

The problem of continuum mechanics modelling of lattices was considered in the 2-D formulation, and this is relevant for a number of material systems (such as 2-D colloids, graphene, boron nitride, etc.). However, the general conclusions reached on limitations of such modelling are relevant for 3-D lattices as well.

## Note

1. Poisson's ratio for a triangular lattice with the nearest neighbours interactions is equal to  $1/3$ .

## Acknowledgements

The authors are deeply grateful to A.M. Linkov, N.F. Morozov and D.A. Indeitsev for useful discussions.

## Disclosure statement

No potential conflict of interest was reported by the authors.

## Funding

The work of V.A. Kuzkin and A.M. Krivtsov was supported by Russian Science Foundation (V.A. Kuzkin – [15-11-00017], A.M. Krivtsov – [14-11-00599]). The work of E.A. Podolskaya was supported by Russian Foundation for Basic Research [14-01-31487 mol-a].

## References

- [1] J.D. Eshelby, *Distortion of a crystal by point imperfections*, J. Appl. Phys. 25 (1954), pp. 255–261.
- [2] J.D. Eshelby, *The continuum theory of lattice defects*, Solid State Phys. 3 (1956), pp. 79–144.
- [3] J.D. Eshelby, *The determination of the elastic field of an ellipsoidal inclusion, and related problems*, Proc. R. Soc. A 241 (1957), pp. 376–396.
- [4] R. Bonnet and S. Neily, *An anisotropic thin crystal deformed by an inclined dislocation*, Philos. Mag. 95 (2015), pp. 2764–2776.
- [5] R.V. Goldstein and N.F. Morozov, *Mechanics of deformation and fracture of nanomaterials and nanotechnology*, Phys. Mesomech. 10 (2007), pp. 235–246.
- [6] L. Pizzagalli, S. Brochard, J. Godet, and C. Gérard, *Mechanical Properties of Nanostructure*, in *Encyclopedia of Nanotechnology*, B. Bhushan, ed., Springer, Dordrecht, 2015, pp. 1–11.
- [7] A.M. Krivtsov and N.F. Morozov, *On mechanical characteristics of nanocrystals*, Phys. Solid State 44 (2002), pp. 2260–2265.
- [8] V.A. Eremeyev, *On effective properties of materials at the nano- and microscales considering surface effects*, Acta Mech. 227 (2016), pp. 29–42.
- [9] H. Kanzaki, *Point defects in face-centred cubic lattice — I distortion around defects*, J. Phys. Chem. Solids 2 (1957), pp. 24–36.
- [10] J.W. Flocken, *Modified lattice-statics approach to point-defect calculations*, Phys. Rev. B 6 (1972), pp. 1176–1181.
- [11] J.R. Hardy, *A theoretical study of point defects in the rocksalt structure substitutional K<sup>+</sup> in NaCl*, J. Phys. Chem. Solids 15 (1960), pp. 39–49.
- [12] J.R. Hardy and R. Bullough, *Point defect interactions in harmonic cubic lattices*, Philos. Mag. 15 (1967), pp. 237–246.
- [13] J.W. Flocken and J.R. Hardy, *Application of the method of lattice statics to interstitial Cu atoms in Cu*, Phys. Rev. 175 (1968), pp. 919–927.
- [14] J.W. Flocken and J.R. Hardy, *Application of the method of lattice statics to vacancies in Na, K, Rb, and Cs*, Phys. Rev. 177 (1969), pp. 1054–1062.

- [15] J.W. Flocken and J.R. Hardy, *Asymptotic lattice displacements about point defects in cubic metals*, Phys. Rev. B 1 (1970), pp. 2447–2456.
- [16] K.M. Miller and P.T. Heald, *The lattice distortion around a vacancy in FCC metals*, Phys. Status Solidi B 67 (1975), pp. 569–576.
- [17] S.K. Rattan, P. Singh, S. Prakash, and J. Singh, *Strain field due to point defects in metals*, Phys. Rev. B 47 (1993), pp. 599–607.
- [18] A.J.E. Foreman, *Elastic relaxation at a vacancy in solid argon*, Philos. Mag. 8 (1963), pp. 1211–1217.
- [19] A. Yavari, M. Ortiz, and K. Bhattacharya, *A theory of anharmonic lattice statics for analysis of defective crystals*, J. Elast. 86 (2007), pp. 41–83.
- [20] S. Kavianpour and A. Yavari, *Anharmonic analysis of defective crystals with many-body interactions using symmetry reduction*, Comput. Mater. Sci. 44 (2009), pp. 1296–1306.
- [21] V.K. Tewary, *Green-function method for lattice statics*, Adv. Phys. 22 (1973), pp. 757–810.
- [22] R. Thomson and S.J. Zhou, *Interfacial crack in a two-dimensional hexagonal lattice*, Phys. Rev. B 49 (1994), pp. 44–54.
- [23] X. Liu and N. Liang, *Effective elastic moduli of triangular lattice material with defects*, J. Mech. Phys. Solids 60 (2012), pp. 1722–1739.
- [24] B. Yang and V.K. Tewary, *Green's function-based multiscale modeling of defects in a semi-infinite silicon substrate*, Int. J. Solids Struct. 42 (2005), pp. 4722–4737.
- [25] B. Yang and V.K. Tewary, *Multiscale Green's function for the deflection of graphene lattice*, Phys. Rev. B 77 (2008), pp. 245442-1–245442-5.
- [26] R. Migoni, C.N. Tome, N. Smetniansky-De Grande, and E.J. Savino, *Lattice static Green function for an hcp lattice*, Phys. Rev. B 22 (1980), pp. 2658–2664.
- [27] W. Lechner, E. Scholl-Paschinger, and C. Dellago, *Displacement fields of point defects in two-dimensional colloidal crystals*, J. Phys.-Condens. Matter 20 (2008), p. 404202 (7pp).
- [28] W. Lechner and C. Dellago, *Point defects in two-dimensional colloidal crystals: simulation vs. elasticity theory*, Soft Matter 5 (2009), pp. 646–659.
- [29] H. Cong, B. Yu, S. Wang, L. Qi, J. Wang, and Y. Ma, *Preparation of iridescent colloidal crystal coatings with variable structural colors*, Opt. Express 21 (2013), pp. 17831–17838.
- [30] B. van der Meer, W. Qi, J. Sprakel, L. Fillion, and M. Dijkstra, *Dynamical heterogeneities and defects in two-dimensional soft colloidal crystals*, Soft Matter 11 (2015), pp. 9385–9392.
- [31] M. Shariyat, Z. Sarvi, and M. Asgari, *A unit-cell-based three-dimensional molecular mechanics analysis for buckling load, effective elasticity and Poisson's ratio determination of the nanosheets*, Mol. Simulat. 42 (2016), pp. 353–369.
- [32] N.I. Muskhelishvili, *Some Basic Problems of the Mathematical Theory of Elasticity*, Groningen, Noordhoff, 1953.
- [33] L. Filshinskii and E. Grigoliuk, *Perforated Plates and Shells*, Nauka, Moscow, 1970. Russian.
- [34] A.M. Linkov, *Boundary Integral Equations in Elasticity Theory*, Kluwer Academic Publishers, Dordrecht, 2002.
- [35] B.L. Karihaloo and J. Wang, *On the solution of doubly periodic array of cracks*, Mech. Mater. 26 (1997), pp. 209–212.
- [36] A.A. Kelly and K.M. Knowles, *Crystallography and Crystal Defects*, 2nd ed., John Wiley and Sons Ltd, Chichester, 2012.
- [37] R. Thomson, S.J. Zhou, A.E. Carlsson, and V.K. Tewary, *Lattice imperfections studied by use of lattice Green's functions*, Phys. Rev. B 46 (1992), pp. 10613–10622.
- [38] R.P. Agarwal, *Difference Equations and Inequalities*, Marcel Dekker, New York, 2000.
- [39] A. Metsue, A. Oudriss, and X. Feugas, *Displacement field induced by a vacancy in nickel and some implications for the solubility of hydrogen*, Philos. Mag. 94 (2014), pp. 3978–3991.
- [40] W. Lechner, D. Polster, G. Maret, P. Keim, and C. Dellago, *Self-organized defect strings in two-dimensional crystals*, Phys. Rev. E 88 (2013), pp. 060402-1–060402-4.
- [41] L. Verlet, *Computer "experiments" on classical fluids. I. Thermodynamical properties of Lennard-Jones molecules*, Phys. Rev. 159 (1967), pp. 98–103.
- [42] S.K. Kanaun and V. Levin, *Self-consistent Methods for Composites*, Static Problems Vol. 1, Netherlands, Springer, 2007.



- [43] M. Kachanov, I. Tsukrov, and B. Shafiro, *Effective moduli of solids with cavities of various shapes*, Appl. Mech. Rev. 47 (1994), pp. S151–S174.
- [44] T.C. Ekneligoda and R.W. Zimmerman, *Compressibility of two-dimensional pores having n-fold axes of symmetry*, Proc. R. Soc. A 462 (2006), pp. 1933–1947.
- [45] T.C. Ekneligoda and R.W. Zimmerman, *Shear compliance of two-dimensional pores possessing N-fold axis of rotational symmetry*, Proc. R. Soc. A 464 (2008), pp. 759–775.
- [46] A.M. Krivtsov and M. Wiercigroch, *Molecular dynamics simulation of mechanical properties for polycrystal materials*, Mater. Phys. Mech. 3 (2001), pp. 45–51.
- [47] V.A. Kuzkin, A.M. Krivtsov, R.E. Jones, and J.A. Zimmerman, *Material frame representation of equivalent stress tensor for discrete solids*, Phys. Mesomech. 18 (2015), pp. 13–23.
- [48] V.A. Kuzkin, *Interatomic force in systems with multibody interactions*, Phys. Rev. E 82 (2010), pp. 016704-1–016704-6.
- [49] T.C. Ekneligoda and R.W. Zimmerman, *Boundary perturbation solution for nearly circular holes and rigid inclusions in an infinite elastic medium*, J. Appl. Mech. 75 (2008), p. 011015 (8pp).

## Appendix 1. General solution of a discrete doubly periodic problem

Consider the general solution of the discrete doubly periodic problem (8), (9). Substituting (9) into the equilibrium Equations (8) yields the equations with respect to doubly periodic function  $\tilde{\mathbf{u}}^{n,m}$ :

$$\begin{aligned} (\Delta_u - \beta_u^+ - \beta_u^-)\tilde{u}^{n,m} + (\Delta_w - \beta_w^+ - \beta_w^-)(\tilde{u}^{n,m} + \tilde{v}^{n,m}) &= d_u + d_w, \\ (\Delta_v - \beta_v^+ - \beta_v^-)\tilde{v}^{n,m} + (\Delta_w - \beta_w^+ - \beta_w^-)(\tilde{u}^{n,m} + \tilde{v}^{n,m}) &= d_v + d_w, \\ n, m &= -N, \dots, N, \end{aligned} \quad (\text{A1})$$

where

$$\begin{aligned} d_u &= \varepsilon_u a(\delta^{n-1,m} - \delta^{n+1,m}), \quad d_v = \varepsilon_v a(\delta^{n,m-1} - \delta^{n,m+1}), \\ d_w &= \varepsilon_w a(\delta^{n-1,m-1} - \delta^{n+1,m+1}), \quad \varepsilon_s = \mathbf{e}_s \cdot \boldsymbol{\varepsilon} \cdot \mathbf{e}_s, \quad s = u, v, w. \end{aligned} \quad (\text{A2})$$

Thus, we obtain a system of  $2(2N + 1)^2$  equations for the displacements. Due to the fact that  $\tilde{\mathbf{u}}^{n,m}$  is a doubly periodic function, it is convenient to seek the solution of (A1) using the DFT. This allows to satisfy the conditions of double periodicity (9) automatically. The direct and inverse DFTs have the forms:

$$\begin{aligned} Z^{s,p} = \Phi(z^{n,m}) &= \sum_{n,m=-N}^N z^{n,m} \xi^{-sn-mp}, \quad \xi = e^{i\theta}, \quad \theta = \frac{2\pi}{2N+1}, \\ z^{n,m} = \Phi^{-1}(Z^{s,p}) &= \frac{1}{(2N+1)^2} \sum_{s,p=-N}^N Z^{s,p} \xi^{sn+mp}, \end{aligned} \quad (\text{A3})$$

where  $i$  is the imaginary unit. Thus, the system of equations for the Fourier images  $U^{s,p} = \Phi(u^{n,m})$ ,  $V^{s,p} = \Phi(v^{n,m})$  yields:

$$\begin{aligned} \left( \sin^2 \frac{s\theta}{2} + \sin^2 \frac{(s+p)\theta}{2} \right) U^{s,p} + \sin^2 \frac{(s+p)\theta}{2} V^{s,p} &= Q_1, \\ \sin^2 \frac{(s+p)\theta}{2} U^{s,p} + \left( \sin^2 \frac{p\theta}{2} + \sin^2 \frac{(s+p)\theta}{2} \right) V^{s,p} &= Q_2, \end{aligned} \quad (\text{A4})$$

where  $Q_1, Q_2$ :

$$\begin{aligned} Q_1 &= Y^{s,p} - \frac{ia}{2} (\varepsilon_u \sin s\theta + \varepsilon_w \sin (s+p)\theta), \\ Q_2 &= Y^{p,s} - \frac{ia}{2} (\varepsilon_v \sin p\theta + \varepsilon_w \sin (s+p)\theta), \\ Y^{s,p} &= \frac{1}{4} [\tilde{w}^{1,1}(\xi^{-p-s} - 1) + \tilde{w}^{-1,-1}(\xi^{p+s} - 1) + \tilde{u}^{1,0}(\xi^{-s} - 1) + \tilde{u}^{-1,0}(\xi^s - 1)]. \end{aligned} \quad (\text{A5})$$

Note, that, if  $s = p = 0$ , the equations hold identically, hence,  $U^{0,0}, V^{0,0}$  are arbitrary. The determinant of the system is:

$$D^{s,p} = \sin^2 \frac{s\theta}{2} \sin^2 \frac{p\theta}{2} + \sin^2 \frac{p\theta}{2} \sin^2 \frac{(s+p)\theta}{2} + \sin^2 \frac{s\theta}{2} \sin^2 \frac{(s+p)\theta}{2}. \quad (\text{A6})$$

Solving the equations for images and using the inverse DFT, we obtain the doubly periodic part of the displacements:

$$\begin{aligned} \tilde{u}^{n,m} &= \Phi^{-1} \left( \frac{1}{D^{s,p}} \left[ Q_1 \left( \sin^2 \frac{p\theta}{2} + \sin^2 \frac{(s+p)\theta}{2} \right) - Q_2 \sin^2 \frac{(s+p)\theta}{2} \right] \right), \\ \tilde{v}^{n,m} &= \Phi^{-1} \left( \frac{1}{D^{s,p}} \left[ Q_2 \left( \sin^2 \frac{s\theta}{2} + \sin^2 \frac{(s+p)\theta}{2} \right) - Q_1 \sin^2 \frac{(s+p)\theta}{2} \right] \right). \end{aligned} \quad (\text{A7})$$

Formula (A7) gives the general solution of the discrete doubly periodic problem for a triangular lattice with vacancies.

## Appendix 2. Displacement field in the case of volumetric mean strain

Let us calculate the displacement field around a vacancy in the case of volumetric mean strain:

$$\boldsymbol{\varepsilon} = \varepsilon \mathbf{I}, \quad \varepsilon_u = \varepsilon_v = \varepsilon_w = \varepsilon. \quad (\text{B8})$$

Due to symmetry of the problem, displacements of the particles that surround the vacancy satisfy the identities:

$$\tilde{\mathbf{u}}^{1,0} = -\tilde{\mathbf{u}}^{-1,0} = \tilde{u}^{1,0} \mathbf{e}_u, \quad \tilde{\mathbf{u}}^{0,1} = -\tilde{\mathbf{u}}^{0,-1} = \tilde{u}^{1,0} \mathbf{e}_v, \quad \tilde{\mathbf{u}}^{1,1} = -\tilde{\mathbf{u}}^{-1,-1} = \tilde{u}^{1,0} \mathbf{e}_w. \quad (\text{B9})$$

Thus, the right parts of (A4) have the form:

$$Q_1(s, p) = -\frac{i(a\varepsilon + \tilde{u}^{1,0})}{2} [\sin s\theta + \sin (s+p)\theta], \quad Q_2(s, p) = Q_1(p, s). \quad (\text{B10})$$

Solving (A4) with the use of (B10) and the inverse DFT, we obtain:

$$\begin{aligned} \tilde{u}^{n,m} &= \tilde{v}^{m,n} = -(a\varepsilon + \tilde{u}^{1,0}) G^{n,m}, \\ G^{n,m} &= \frac{1}{2(2N+1)^2} \sum_{s,p=-N}^N \frac{\sin((sn+pm)\theta)}{D^{s,p}} \left( \sin p\theta \sin^2 \frac{s\theta}{2} - \sin s\theta \sin^2 \frac{(s+p)\theta}{2} \right). \end{aligned} \quad (\text{B11})$$

In order to exclude  $\tilde{u}^{1,0}$ , we substitute  $n = 1, m = 0$ . Finally, the displacement field in the triangular lattice with doubly periodic system of vacancies under volumetric mean strain has the form:

$$u^{n,m} = v^{m,n} = a\varepsilon \left( n - \frac{m}{2} - \frac{G^{n,m}}{1 + G^{1,0}} \right). \quad (\text{B12})$$

### Appendix 3. Displacement field in the case of biaxial mean strain

Let us calculate the displacement field in the case of biaxial mean strain along the orthogonal directions  $\mathbf{i} = (\mathbf{e}_u - \mathbf{e}_v)/\sqrt{3}$  and  $\mathbf{j} = \mathbf{e}_u + \mathbf{e}_v$ . The mean strain tensor is given by:

$$\boldsymbol{\varepsilon} = \frac{\varepsilon_{xx}}{3}(\mathbf{e}_u - \mathbf{e}_v)(\mathbf{e}_u - \mathbf{e}_v) + \varepsilon_{yy}\mathbf{e}_w\mathbf{e}_w, \quad \varepsilon_u = \varepsilon_v = \frac{3\varepsilon_{xx} + \varepsilon_{yy}}{4}, \quad \varepsilon_w = \varepsilon_{yy}. \quad (\text{C13})$$

Due to symmetry of the problem, displacements of the particles that surround the vacancy satisfy the identities:

$$\tilde{u}^{1,0} = -\tilde{u}^{-1,0}, \quad \tilde{v}^{0,1} = -\tilde{v}^{0,-1}, \quad \tilde{u}^{1,0} = \tilde{v}^{0,1}, \quad \tilde{w}^{1,1} = -\tilde{w}^{-1,-1}. \quad (\text{C14})$$

The displacements  $\tilde{u}^{1,0}$ ,  $\tilde{w}^{1,1}$  are independent variables. The right parts of (A4) yield:

$$Q_1(s, p) = Q_2(p, s) = -\frac{i}{2} [(a\varepsilon_u + \tilde{u}^{1,0}) \sin s\theta + (a\varepsilon_w + \tilde{w}^{1,1}) \sin (s + p)\theta]. \quad (\text{C15})$$

Hence, the doubly periodic part of the displacements has the form:

$$\tilde{u}^{n,m} = \tilde{v}^{m,n} = H^{n,m}(a\varepsilon_u + \tilde{u}^{1,0}) + K^{n,m}(a\varepsilon_w + \tilde{w}^{1,1}), \quad (\text{C16})$$

where  $H^{n,m}, K^{n,m}$  are defined by formula (19). Substituting  $n = 1, m = 0$  and  $n = 1, m = 1$  into (C16) yields a system of equations for  $\tilde{u}^{1,0}, \tilde{w}^{1,1}$ . The solution of this system is:

$$\begin{aligned} \tilde{u}^{1,0} &= a \frac{(H^{1,0}(1 - 2K^{1,1}) + 2H^{1,1}K^{1,0})\varepsilon_u + K^{1,0}\varepsilon_w}{(1 - H^{1,0})(1 - 2K^{1,1}) - 2K^{1,0}H^{1,1}}, \\ \tilde{w}^{1,1} &= 2a \frac{H^{1,1}\varepsilon_u + (K^{1,1}(1 - H^{1,0}) + H^{1,1}K^{1,0})\varepsilon_w}{(1 - H^{1,0})(1 - 2K^{1,1}) - 2K^{1,0}H^{1,1}}. \end{aligned} \quad (\text{C17})$$

Thus, substitution of (C17) and (9) into (C16) gives the displacement field in the crystal with vacancies under biaxial strain. Note that coefficients in the formulae (C16), (C17) depend only on the distance between the vacancies, i.e. on the parameter  $N$ .